

STRUCTURAL ERROR PATTERNS MATTER: TOWARDS MORE STRUCTURE-AWARE GNN EVALUATION AND TRAINING

006 **Anonymous authors**

007 Paper under double-blind review

ABSTRACT

013 Graph Neural Networks (GNNs) are a specialized family of neural networks de-
 014 signed to handle graph-structured data, enabling the modeling of complex rela-
 015 tionships within graphs. Despite significant algorithmic improvements, the issue
 016 of performance evaluation for GNNs has largely been overlooked in the literature.
 017 A crucial but underexplored aspect of GNN evaluation is understanding how er-
 018 rors are distributed across the graph structure, which we refer to as the “structural
 019 error pattern”. To the best of our knowledge, this paper is among the first to high-
 020 light the importance of paying attention to these error patterns, which are essential
 021 not only for model selection—especially in spatial applications where localized or
 022 clustered errors can signal critical issues—but also for providing algorithmic in-
 023 sights into the model’s performance. In this work, we introduce a novel mathemat-
 024 ical framework that analyzes and differentiates evaluation metrics based on their
 025 sensitivity to structural error patterns. Through a thorough theoretical analysis, we
 026 identify the limitations of traditional metrics—such as accuracy and mean squared
 027 error—that fail to capture the complexity of these error distributions. To address
 028 these shortcomings, we propose a new evaluation metric explicitly designed to
 029 detect and quantify structural error patterns, offering deeper insights into GNN
 030 performance. Our extensive empirical experiments demonstrate that this metric
 031 enhances model selection and improves robustness. Furthermore, we show that it
 032 can be incorporated as a regularization method during training, leading to more
 033 reliable GNN predictions in real-world applications.

1 INTRODUCTION

036 Graph Neural Networks (GNNs) have emerged as powerful models for analyzing graph-structured
 037 data, thanks to their ability to capture complex relational dependencies inherent in graph topolo-
 038 gies. This makes GNNs particularly effective for node-level prediction tasks, such as classifica-
 039 tion or regression, where the target prediction is associated with individual nodes and influenced by their
 040 structural context and interactions with neighboring entities. As a result, GNNs have achieved sig-
 041 nificant success across a wide range of applications, including traffic forecasting (Zhao et al., 2019a;
 042 Guo et al., 2019; Zhang et al., 2020; Jiang & Luo, 2022), urban planning (Li et al., 2022; Chen,
 043 2020), environmental monitoring (Zhang et al., 2023; Li et al., 2024), social network analysis (Kipf
 044 & Welling, 2017), and sensor network analysis (Dong et al., 2023; Saadati et al., 2024). In these
 045 contexts, data naturally form graphs, where nodes represent the entities of interest, and edges capture
 046 relationships such as proximity or connectivity. By integrating local node features with structural
 047 relationships across the graph, GNNs can deliver accurate, context-aware predictions that reflect the
 underlying structural dynamics and dependencies.

048 **Existing Gaps.** Most research on GNNs has focused on algorithmic innovations, architectural im-
 049 provements, and system optimizations, aiming to enhance computational efficiency, scalability, or
 050 predictive performance. However, comparatively little attention has been given to developing evalua-
 051 tion metrics specifically tailored for network applications Bechler-Speicher et al. (2025). Rigorous
 052 evaluation frameworks are essential for reliably assessing model performance and guiding model
 053 selection, which directly impacts practical deployment and real-world effectiveness (Shchur et al.,
 2018; Dwivedi et al., 2023). In particular, for network applications, appropriate metrics should

not only quantify predictive accuracy but also capture critical characteristics of error distributions, such as clustering or dispersion patterns. **Without structure-aware evaluation, practitioners lack insights into how prediction errors manifest across the graph, hindering their ability to diagnose, address, and prevent localized failures effectively. Moreover, as demonstrated in (Huang et al.) and in this paper, structural error patterns provide valuable insights for improving GNN frameworks.**

Limitations of Existing Evaluation Metrics. Currently, GNN model evaluation predominantly relies on traditional metrics—such as accuracy (ACC) for node classification or mean squared error (MSE) for node regression tasks. While these metrics are widely adopted, they evaluate predictions independently at each node, ignoring the structural context and inter-node dependencies that are inherent to graph datasets. As we demonstrate both theoretically and empirically in this paper, such metrics fail to distinguish between different structural error patterns, including clustered errors and errors that are randomly distributed across the graph. This limitation is particularly problematic for real-time and fault-tolerant network systems. For instance, in traffic monitoring, where the graph structure represents spatial connectivity, clustered prediction errors may indicate localized congestion or sensor malfunctions that require immediate attention, whereas randomly dispersed errors may simply reflect minor inaccuracies (Xu et al., 2024; Fathurrahman & Gautama, 2024; Moretti et al., 2025). We illustrate this limitation further through a quantitative example in Appendix D.1. Consequently, the inability of conventional metrics to detect these structural error patterns significantly restricts practitioners’ capacity for timely identification and intervention in critical regions. **Thus, developing evaluation frameworks explicitly designed to capture and quantify structural error distributions in GNN predictions is both urgent and essential.**

Contributions. In this paper, we address the under-explored yet crucial aspect of evaluating GNNs within network applications. Specifically, we examine widely used evaluation metrics and identify their inadequacies in capturing structural prediction error patterns. To overcome these limitations, we propose a novel structure-aware evaluation metric explicitly designed to quantify and differentiate structural error patterns, enabling precise detection of structural clustering in prediction errors. The key contributions and findings of this paper are summarized as follows:

- We develop a comprehensive mathematical framework to analyze evaluation metrics commonly employed in GNN tasks. Extending the concept of *expressiveness* (Definition 1), originally introduced in the context of the graph isomorphism problem, we formally define and analyze the property of *exchangeability* (Definition 2) inherent in traditional metrics such as ACC and MSE. Through rigorous theoretical analysis, we demonstrate critical limitations of exchangeable metrics, particularly their inability to differentiate distinct structural error patterns, such as clustered, dispersed, or randomly distributed errors (Theorem 3.1). This fundamental shortcoming emphasizes the necessity for metrics explicitly tailored to capturing structural error distributions in GNN predictions.
- Motivated by our theoretical insights, we propose a novel structure-aware evaluation metric, termed **Structural Cluster Statistic (SCS)**. SCS quantifies structural autocorrelation among prediction errors, effectively identifying structurally clustered error patterns. This metric complements existing evaluation methods by providing deeper insights into structurally predictive behaviors, thereby improving both model selection and interpretability in network-structured tasks.
- Beyond evaluation, we demonstrate how our SCS metric can be adapted into a regularization framework during model training. Specifically, we introduce the **Structural-Cluster-Aware (SCA)** learning objective, an extension of SCS designed to explicitly regularize structural error distributions. Incorporating SCA encourages GNNs to yield predictions with fewer structurally clustered errors, which is especially advantageous for critical network/graph applications requiring robust and reliable performance, such as real-time fault-tolerant network systems.
- We extensively validate our proposed metric and regularization approach through empirical studies involving multiple benchmark and synthetic datasets, as well as representative GNN architectures. Our results yield several important findings: (1) existing GNN models consistently exhibit structurally clustered prediction errors, highlighting the inadequacy of traditional evaluation metrics; (2) distinct structural error patterns are significantly influenced by the underlying graph structure (e.g., regular versus power-law connectivity) rather than by architectural differences among GNN variants; (3) our SCA regularization method effectively mitigates structural error clustering, significantly enhancing the structural robustness and reliability of GNN predictions.

108

2 PRELIMINARY AND BACKGROUND

110 **Graph Data and Network Applications.** A graph is formally defined as $\mathcal{G} = (\mathcal{V}, \mathcal{E})$, where $\mathcal{V} =$
 111 $\{v_1, v_2, \dots, v_n\}$ denotes the set of nodes (vertices), and $\mathcal{E} \subseteq \mathcal{V} \times \mathcal{V}$ represents the set of edges that
 112 capture relationships or interactions between nodes. Each node $v \in \mathcal{V}$ is associated with a feature
 113 vector $\mathbf{x}_v \in \mathbb{R}^d$, encoding relevant attributes or measurements specific to that node. In network
 114 applications, prediction tasks are commonly defined at the node level, with each node assigned a
 115 label $y_v \in \mathcal{Y}$. For instance, in environmental monitoring scenarios, the goal might be to classify each
 116 node based on pollution intensity (e.g., low, moderate, or high) using node-specific measurements.
 117 The primary objective is therefore to learn a predictive model that effectively integrates local node
 118 features and graph topology to accurately predict individual node labels. Additionally, we denote the
 119 adjacency matrix as \mathbf{A} , the degree matrix as \mathbf{D} and the graph Laplacian and normalized Laplacian
 120 matrices as $\mathbf{L} = \mathbf{D} - \mathbf{A}$ and $\hat{\mathbf{L}} = \mathbf{D}^{-1/2} \mathbf{L} \mathbf{D}^{-1/2}$, respectively.

121 **Graph Neural Networks (GNNs).** GNN models broadly fall into three families based on their
 122 approaches for capturing graph structures: *message-passing (spatial-based)*, *spectral-based*, and
 123 *graph transformer* methods (see Appendix A for a more detailed introduction and discussion).
 124 Message-passing GNNs capture dependencies by iteratively aggregating and updating node em-
 125 beddings based on local neighborhood information. These models naturally encode local graph
 126 structures without explicit spectral decomposition, making them computationally efficient and in-
 127 tuitive. Spectral-based GNNs define graph convolution operations via spectral filtering based on
 128 the eigen-decomposition of the graph Laplacian. They effectively capture global graph structures
 129 but often require computationally efficient approximations due to complexity constraints. Graph
 130 transformers extend the spatial approach by incorporating self-attention mechanisms, dynamically
 131 adapting the weights of neighboring nodes. This method allows flexible modeling of both local and
 132 global dependencies and often uses positional encodings to further enhance node representations.

133 **Performance Evaluation of GNNs.** The performance evaluation of GNN models is typically car-
 134 ried out on a dedicated test set, denoted as $\mathcal{V}_{\text{test}} = \{v_1, v_2, \dots, v_k\} \subset \mathcal{V}$. Ground-truth labels for
 135 these nodes are represented as $\mathcal{Y}_{\text{test}} = \{y_1, y_2, \dots, y_k\}$, while the predictions from the GNN model
 136 are denoted by $\hat{\mathcal{Y}} = \{\hat{y}_1, \hat{y}_2, \dots, \hat{y}_k\}$. The evaluation involves quantifying discrepancies between
 137 predicted and true labels using an appropriate performance metric. Formally, given a complete vec-
 138 tor of ground-truth labels $\mathbf{Y} = [y_1, y_2, \dots, y_k]$ and corresponding predictions $\hat{\mathbf{Y}} = [\hat{y}_1, \hat{y}_2, \dots, \hat{y}_k]$,
 139 we define the error vector ϵ as:

$$140 \quad \epsilon = (\epsilon_1, \dots, \epsilon_k), \quad \epsilon_i = f(y_i, \hat{y}_i),$$

141 where $f(\cdot)$ denotes a pointwise loss function that measures the deviation or severity of the prediction
 142 error. Typical examples include the square error $f(y_i, \hat{y}_i) = (y_i - \hat{y}_i)^2$ for regression tasks, or the
 143 misclassification indicator $f(y_i, \hat{y}_i) = \mathbb{I}(y_i \neq \hat{y}_i)$ for classification tasks.

146

3 MAIN RESULTS

148 In this section, we present our main results. We first introduce a mathematical framework that allows
 149 us to formally analyze the capability of evaluation metrics, highlighting critical limitations inherent
 150 in commonly used metrics. Based on these insights, we propose a novel structure-aware evaluation
 151 metric inspired by Moran’s I statistic Moran (1950), and demonstrate how it can also serve as a
 152 regularizer during the training process.

154

3.1 LIMITATIONS OF CURRENT EVALUATION METRICS

155 We first introduce a formal framework to rigorously characterize the capability of evaluation metrics
 156 to differentiate distinct structural error patterns. Inspired by the concept of expressive power in GNN
 157 literature, we define the expressiveness of an evaluation metric as its ability to distinguish between
 158 different error distributions in expectation:

159 **Definition 1** (Distribution Expressiveness of Evaluation Metrics). *Let $\mu(\cdot)$ be an evaluation metric
 160 mapping the error vector ϵ to a real value. Given two distinct error distributions \mathbb{P}_1 and \mathbb{P}_2 , we say
 161 the evaluation metric μ can differentiate between these distributions if $\mathbb{E}_{\mathbb{P}_1}[\mu(\epsilon)] \neq \mathbb{E}_{\mathbb{P}_2}[\mu(\epsilon)]$.*

162 This definition allows us to formally evaluate how well existing metrics capture meaningful differences
 163 in structural error distributions. Next, we introduce a key property commonly exhibited by
 164 traditional metrics used in evaluating GNN performance.

165 **Definition 2** (Exchangeable Measure). *For a graph with N nodes, an evaluation metric $\mu(\cdot)$ is said
 166 to be exchangeable if, for any permutation π of node indices $\{1, 2, \dots, N\}$, it holds that:*

$$167 \quad \mu(\epsilon) = \mu(\pi(\epsilon)), \quad \text{where} \quad \pi(\epsilon) = [\epsilon_{\pi(1)}, \epsilon_{\pi(2)}, \dots, \epsilon_{\pi(N)}].$$

169 Intuitively, exchangeability implies that the metric’s evaluation does not depend on the ordering of
 170 errors but only on their multiset. Conventional metrics for evaluating GNN performance (e.g., ACC,
 171 MSE, F1-score, AU-ROC) satisfy this definition. For instance, ACC, defined as:

$$172 \quad \mu_{\text{ACC}}(\epsilon) = \frac{1}{N} \sum_{i=1}^N \mathbb{I}(\epsilon_i = 0),$$

175 where $\mathbb{I}(\cdot)$ is an indicator function, clearly remains unchanged under any permutation π of the node
 176 indices:

$$177 \quad \mu_{\text{ACC}}(\epsilon) = \frac{1}{N} \sum_{i=1}^N \mathbb{I}(\epsilon_i = 0) = \frac{1}{N} \sum_{i=1}^N \mathbb{I}(\epsilon_{\pi(i)} = 0) = \mu_{\text{AP}}(\pi(\epsilon)).$$

178 Thus, ACC is exchangeable, and similar reasoning can be applied to other common evaluation
 179 metrics. However, exchangeable metrics inherently face critical limitations, which we formalize in the
 180 following theorem:

181 **Theorem 3.1** (Limitation of Exchangeable Metrics). *Let \mathbb{P}_1 and \mathbb{P}_2 be two distinct error distributions
 182 for a GNN on a given graph \mathcal{G} . Suppose $\mu(\cdot)$ is an exchangeable evaluation metric. Then,*

$$183 \quad \mathbb{E}_{\mathbb{P}_1}[\mu(\epsilon)] = \mathbb{E}_{\mathbb{P}_2}[\mu(\epsilon)], \quad \text{provided that} \quad \mathbb{E}_{\mathbb{P}_1}[S(\epsilon)] = \mathbb{E}_{\mathbb{P}_2}[S(\epsilon)],$$

184 where $S(\epsilon) = \sum_{v \in \mathcal{V}} f(y_v, \hat{y}_v)$.

185 Theorem 3.1 indicates that exchangeable metrics cannot distinguish between error patterns if the
 186 total magnitude or frequency of errors is identical, regardless of how those errors are distributed
 187 over the graphs. These metrics treat errors merely as interchangeable entities, failing to account
 188 for their topological arrangement on the graph. Consequently, such metrics are insufficient for
 189 evaluating GNNs predictive performance, especially in applications where the structure of errors
 190 carries critical information.

191 **Concrete Examples.** To illustrate these theoretical limitations more concretely, consider two models
 192 predicting traffic flow in a network, with different error distributions. In the first model, errors are
 193 uniformly distributed across the network with larger individual errors. In the second model, smaller
 194 errors occur, but they are concentrated at specific critical locations. Traditional metrics, such as
 195 MSE, would favor the second model due to its lower average error. However, these metrics fail to
 196 capture the impact of error distribution. Despite smaller average errors, the clustering of errors in
 197 critical areas (e.g., congestion points) can have severe consequences. In contrast, the first model,
 198 though it has larger individual errors, distributes them evenly, leading to a lower risk of localized
 199 failures. This example demonstrates how traditional metrics can overlook critical issues by not
 200 considering the structural distribution of errors. For a detailed quantitative example, see Appendix D.1.

201 Figure 1 provides a visual illustration, where scenarios exhibit identical counts of correct and
 202 incorrect predictions (i.e., same ACC) but vary significantly in structural error patterns, ranging from
 203 clustered to dispersed distributions. As discussed, this variability is critically important in practical
 204 applications such as traffic management or environmental monitoring, where clustered errors
 205 demand urgent attention. The inability of traditional exchangeable metrics to differentiate these
 206 structurally distinct patterns highlights substantial risks associated with model evaluation and de-
 207 ployment decisions based solely on conventional metrics.

208 3.2 STRUCTURAL CLUSTERING STATISTICS (SCS)

209 As illustrated, traditional evaluation metrics typically treat prediction errors independently, neglect-
 210 ing the structural relationships and thus failing to differentiate between randomly distributed errors
 211 and meaningful structural clusters. To address this, we need a metric, which explicitly accounts for
 212 node-to-node relationships within the graph.

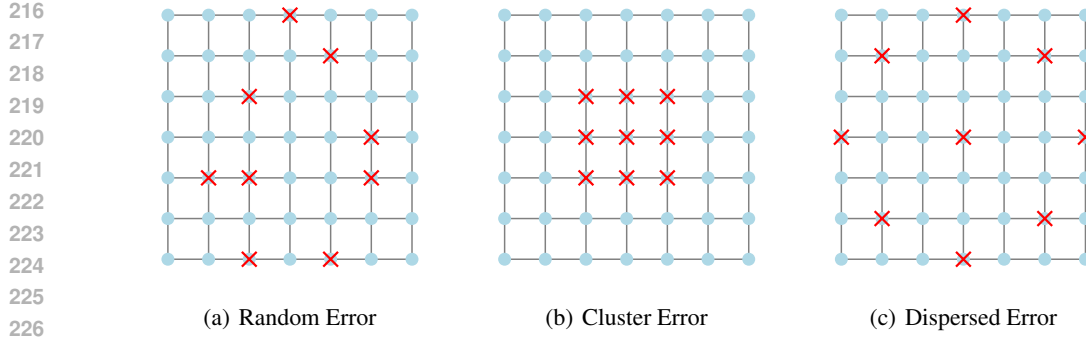


Figure 1: An illustration of distinct structural error patterns. Figure 1(a) (*Random Error*): Incorrect predictions (marked by red crosses) are randomly dispersed across the graph. Figure 1(b) (*Cluster Error*): Incorrect predictions are concentrated within a localized region of the graph. Figure 1(c) (*Dispersed Error*): Incorrect predictions are evenly spaced and distributed apart from one another across the graph. These differing patterns underscore the necessity of using structure-aware evaluation metrics when assessing GNN predictions.

Limitations of Naive Structural Metrics. A straightforward structural evaluation method might measure the structural pattern of errors using average shortest-path distances between incorrectly predicted nodes. However, this naive approach has significant practical limitations. First, it is computationally expensive, particularly for large graphs. Moreover, in graphs with irregular or hub-based structures (e.g., power-law distributed graphs), highly connected nodes disproportionately influence distance-based metrics, obscuring genuine structural clustering patterns and limiting interpretability Barabási (2013).

Formulation of SCS. To address these shortcomings, we introduce the SCS metric, inspired by Moran’s I statistic. SCS quantifies structural autocorrelation by measuring how prediction errors at each node correlate with those of neighboring nodes. This property makes it particularly effective for identifying structural clusters of prediction errors.

Formally, let the prediction error at a test node $v \in \mathcal{V}_{\text{test}}$ be defined as $\epsilon_v = f(y_v, \hat{y}_v)$, where y_v is the ground-truth label and \hat{y}_v is the predicted label generated by the GNN. SCS, computed exclusively over the test set $\mathcal{V}_{\text{test}}$, is given by:

$$\text{SCS}(\epsilon, \mathcal{V}_{\text{test}}) = \frac{k}{W} \frac{\sum_{v,u \in \mathcal{V}_{\text{test}}} w_{vu}(\epsilon_v - \bar{\epsilon})(\epsilon_u - \bar{\epsilon})}{\sum_{v \in \mathcal{V}_{\text{test}}} (\epsilon_v - \bar{\epsilon})^2}, \quad (3.1)$$

where $\bar{\epsilon} = 1/k \sum_{v \in \mathcal{V}_{\text{test}}} \epsilon_v$ denotes the mean prediction error across all test nodes, w_{vu} represents the connection weight, $W = \sum_{v,u \in \mathcal{V}_{\text{test}}} w_{vu}$ is the sum of all connection weights over the test set, and $k = |\mathcal{V}_{\text{test}}|$ is the number of nodes in the test set.

SCS explicitly quantifies the correlation of prediction errors among neighboring nodes within the test set. A positive SCS indicates structurally clustered errors, revealing localized regions where the model fails to accurately capture structural dependencies. Values close to zero indicate randomly distributed errors, while negative values imply structurally dispersed error patterns, highlighting discrepancies between model predictions and underlying graph structures. By employing this adapted SCS, we obtain a precise, interpretable, and computationally efficient measure of predictive performance over the graph, thus facilitating targeted model improvements by pinpointing test regions where GNN models exhibit poor structural predictive capabilities.

3.3 STRUCTURAL-CLUSTER-AWARE (SCA) REGULARIZATION

In previous sections, we introduced the SCS as a robust metric for effectively detecting and quantifying structurally clustered errors in GNN predictions. While identifying these error clusters is essential, from a practical standpoint, promoting structurally uniform error distributions is equally critical for real-world network applications. Specifically, structurally correlated prediction errors can propagate rapidly within real-time and fault-tolerant systems—such as environmental sensor

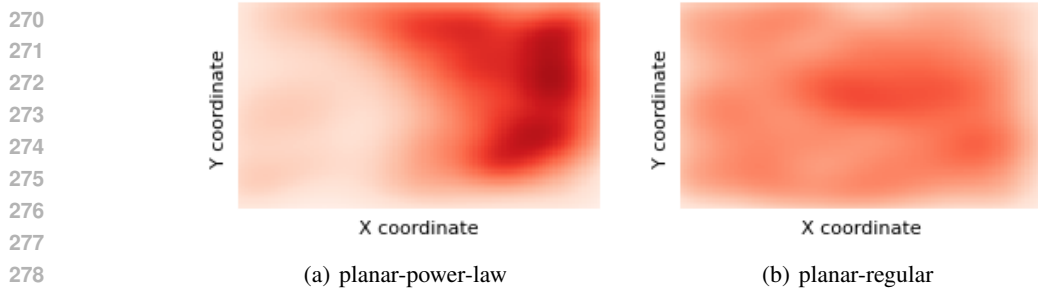


Figure 2: An illustration of structural error patterns in graphs with different structures. The x and y axes represent the coordinates of nodes, and the intensity of the red colour indicates the severity of prediction errors. As shown, the planar-power-law (left) exhibits pronounced structurally clustered errors, whereas the planar-regular (right) displays a more dispersed, uniformly distributed error.

networks, smart grids, and critical infrastructure monitoring—potentially leading to biased predictions, localized failures, and suboptimal decision-making (Zhao et al., 2019b; Chu & Sethu, 2010). Therefore, an important question arises: *can we leverage our proposed structural metric to encourage GNN models to produce more uniformly distributed prediction errors?*

Uniform error distributions offer significant practical benefits. For instance, in environmental monitoring, uniformity reduces the likelihood of systematic regional biases, thereby enhancing reliability, fairness, and accuracy in environmental assessments and policy-making. Similarly, for sensor network deployments, structural uniformity in prediction errors mitigates localized blind spots or overly concentrated error regions, leading to improved overall system resilience and balanced performance across the entire graph domain (Chu & Sethu, 2010).

However, directly employing the original SCS formulation as a regularizer presents notable optimization challenges. Specifically, the original metric can yield negative and unbounded values, complicating gradient-based training and potentially causing numerical instability, especially when prediction variances are small. Minimizing negative structural autocorrelation might inadvertently promote dispersed error patterns rather than uniformity, contradicting the desired optimization goal.

To overcome these limitations, we propose a modified regularization term, Structural-Cluster-Aware (SCA) regularizer. This adjusted form, based on a squared version of the SCS metric, ensures the regularization term is always non-negative and bounded, effectively penalizing significant structural autocorrelation (either clustered or dispersed). Formally, the SCA regularization term is defined as:

$$\mathcal{L}_{\text{SCA}}(\epsilon, \mathcal{G}, \delta) = \left(\frac{k}{W} \frac{\sum_{i,j} w_{ij}(\epsilon_i - \bar{\epsilon})(\epsilon_j - \bar{\epsilon})}{\sum_i (\epsilon_i - \bar{\epsilon})^2 + \delta} \right)^2, \quad (3.2)$$

where all variables are as previously defined. We introduce a small positive constant δ in the denominator to ensure numerical stability, particularly in situations where prediction variance is low, thereby avoiding potential division by zero. In practice, δ is typically chosen as a very small value (e.g., 10^{-6}), minimally influencing the regularization objective while effectively preventing numerical instabilities. The squared formulation of the SCA regularizer guarantees non-negativity, explicitly penalizing significant structural autocorrelation (whether clustered or dispersed). This approach effectively encourages structural uniformity in prediction errors and mitigates localized error clustering. Integrating this structure-aware regularization into the total loss function results in:

$$\mathcal{L}_{\text{total}} = \mathcal{L}_{\text{task}}(\mathbf{Y}, \hat{\mathbf{Y}}) + \lambda \mathcal{L}_{\text{SCA}}(\epsilon, \mathcal{G}, \delta), \quad (3.3)$$

where $\lambda \geq 0$ is a hyperparameter controlling the strength of the structural regularisation. Employing this regularizer encourages structurally consistent predictions, enhances robustness to faults (cluster errors), and ultimately improves the reliability of GNN systems deployed in real-time environments.

4 EMPIRICAL STUDY

In this section, we present an empirical study to investigate the structural characteristics of prediction errors in GNN models. Specifically, we aim to address the following key research questions:

Dataset	Cora		Citeseer		California Housing		Air Temperature	
Model	SCS ↓	ACC(%) ↑	SCS ↓	ACC(%) ↑	SCS ↓	MSE ↓	SCS ↓	MSE ↓
GCN	0.21±0.03	84.4±0.5	0.23±0.03	79.2±0.6	0.14±0.02	0.038±3e-3	0.15±0.03	0.031±2e-3
GCN-SCA	0.10±0.01	84.0±0.4	0.11±0.02	78.8±0.5	0.10±0.01	0.040±2e-3	0.09±0.01	0.033±2e-3
GraphSAGE	0.19±0.02	88.5±0.4	0.20±0.03	80.1±0.4	0.13±0.03	0.041±2e-3	0.16±0.02	0.029±2e-3
GraphSAGE-SCA	0.11±0.01	88.2±0.3	0.13±0.02	79.7±0.4	0.08±0.01	0.042±2e-3	0.10±0.01	0.030±1e-3
GAT	0.18±0.03	88.8±0.3	0.19±0.02	80.4±0.5	0.11±2e-3	0.036±2e-3	0.14±0.01	0.027±1e-3
GAT-SCA	0.08±0.01	88.6±0.4	0.09±0.01	80.1±0.4	0.07±0.01	0.040±1e-3	0.09±0.01	0.029±1e-3
ChebNet	0.25±0.02	86.5±0.4	0.26±0.02	77.8±0.5	0.20±0.02	0.043±2e-3	0.19±0.03	0.032±2e-3
ChebNet-SCA	0.15±0.01	86.2±0.3	0.18±0.01	77.4±0.4	0.12±0.01	0.044±2e-3	0.14±0.02	0.033±2e-3
GraphTransformer	0.15±0.02	89.0±0.3	0.16±0.02	81.2±0.4	0.18±0.02	0.035±2e-3	0.18±0.02	0.027±1e-3
GraphTransformer-SCA	0.07±0.01	88.7±0.3	0.10±0.01	80.9±0.4	0.11±0.01	0.035±1e-3	0.12±0.01	0.028±1e-3
Avg. Improvement (%)	47.96		41.35		36.84		32.92	

Table 1: Evaluation of GNN models with and without the proposed SCA regularization across classification (Cora, Citeseer) and regression (California Housing, Air Temperature) datasets. Models labeled '-SCA' indicate training with our proposed regularization. Lower values (↓) indicate better performance for SCS and Mean Squared Error (MSE), while higher values (↑) indicate better performance for accuracy (ACC). Bold entries highlight improvements achieved by incorporating SCA. The final row summarizes the average percentage of SCS improvement across each dataset, illustrating that SCA effectively mitigates structural clustering in prediction errors.

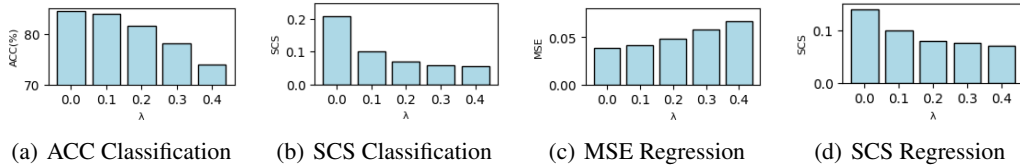


Figure 3: An illustration of the effects of the regularization hyperparameter λ on classification and regression tasks. Figures 3(a) and 3(b) show that increasing λ reduces structural clustering of errors (SCS) but simultaneously decreases classification accuracy (ACC). Similarly, Figures 3(c) and 3(d) illustrate that increasing λ reduces structural clustering in regression errors (SCS) at the expense of increased MSE. Thus, λ effectively manages the trade-off between structural uniformity of errors and overall predictive performance.

1. Do existing GNN models exhibit structurally clustered prediction errors, and if so, how do these clusters differ among various GNN architectures?

2. Is the proposed SCS effective in identifying structurally clustered errors?

3. Can SCA learning effectively mitigate structural clusters in errors?

Implementation details and hyperparameter selections are deferred to the supplementary material.

4.1 EXPERIMENTAL DESIGN

Datasets and Baselines. To comprehensively evaluate our proposed methods across diverse contexts, we select benchmark datasets covering both node classification and regression tasks. Specifically, we use two widely adopted citation network datasets for node classification tasks: *Cora* and *Citeseer*(Sen et al., 2008). For node regression tasks, we use two spatially structured real-world datasets: the *California Housing Prices* datasetPace & Barry (1997) and the *Air Temperature* dataset Hooker et al. (2018). Additionally, to investigate how underlying graph structures influence model performance, we synthesize two planar graph regression datasets characterized by distinct structural patterns: *planar-regular* (uniform degree distribution) and *planar-power-law* (power-law degree distribution). The procedure for synthesis is provided in the supplementary material. For GNNs, we select five representative models covering three prominent categories: message-passing-based GNNs (*GCN*(Kipf & Welling, 2017), *GraphSAGE*(Hamilton et al., 2017), and *GAT*(Veličković et al., 2017)), spectral-based GNNs (*ChebNet*(Defferrard et al., 2016)), and graph transformers (*Graph Transformer*(Dwivedi & Bresson, 2020)). The implementations for these

378 baselines follow widely adopted repositories(Dwivedi et al., 2023; Dwivedi & Bresson, 2020; Hu
 379 et al., 2020), employing standard training procedures and hyperparameter tuning strategies based on
 380 validation sets to ensure fairness.
 381

382 **Evaluation Tasks and Metrics.** We conduct evaluation across two distinct prediction tasks: node
 383 classification and node regression. For classification datasets, we measure performance using ACC,
 384 while for regression datasets, we employ MSE. To evaluate the structural characteristics of predic-
 385 tion errors, we use the proposed SCS. Each GNN model is evaluated under two conditions: with and
 386 without our proposed SCA regularization. For all datasets, we adopt either default data splits (where
 387 provided) or apply a standard random split with a 60%/20%/20% ratio for training, validation, and
 388 testing subsets, respectively. All reported results are averaged over five independent trials, ensuring
 389 statistical robustness and reproducibility.
 390

4.2 EXPERIMENTAL RESULTS

392 **Structural Error Patterns.** Our first set of experiments investigates whether existing GNNs pro-
 393 duce structurally clustered prediction errors and evaluates if our proposed SCS effectively captures
 394 these patterns. Figure 2 illustrates representative structural error distributions on graphs with dif-
 395 ferent underlying structures. Notably, we observe that the graph structure itself, rather than specific
 396 GNN architectures, primarily determines the structural distribution of prediction errors. Specifi-
 397 cally, planar graphs with power-law connectivity tend to exhibit pronounced structurally clustered
 398 errors, while planar graphs with regular connectivity display more uniformly dispersed errors. Given
 399 that many real-world graphs, such as those found in sensor networks or urban infrastructures, of-
 400 ten exhibit scale-free (power-law) characteristics Barabási (2013), our findings suggest that GNNs
 401 deployed in these contexts will typically produce structurally clustered prediction errors. This obser-
 402 vation is quantitatively confirmed by positive SCS values across all evaluated GNN models (Table 1).
 403 The consistency of these results across different architectures further emphasizes that structural clus-
 404 tering is an intrinsic property related to the underlying graph topology rather than being driven solely
 405 by model-specific factors. These findings not only highlight the critical importance of explicitly con-
 406 sidering error structures on the graph in evaluation but also validate the effectiveness of our proposed
 407 SCS metric in identifying and quantifying structural clustering.
 408

408 **Effectiveness of SCA.** We next assess the effectiveness of our proposed SCA regularization
 409 method. Table 1 clearly demonstrates that incorporating SCA significantly reduces structural cluster-
 410 ing of prediction errors (indicated by consistently lower SCS values) across all GNN architectures
 411 and datasets. Particularly notable improvements occur in message-passing-based models such as
 412 GCN, GraphSAGE, and GAT, where structural clustering is substantially reduced by approximately
 413 40%-48%, with only minor degradations in predictive performance (ACC or MSE). Transformer-
 414 based and spectral-based models exhibit slightly smaller reductions, likely due to their inherently
 415 less-clustered baseline error distributions. Nevertheless, these improvements underscore the broad
 416 practical effectiveness of the SCA regularization, particularly valuable for structurally sensitive real-
 417 world applications like environmental monitoring and sensor networks.
 418

418 **Hyperparameter Analysis.** Finally, we conduct a sensitivity analysis on the regularization hy-
 419 perparameter λ , which controls the intensity of the SCA objective. As illustrated in Figure 3, in-
 420 creasing λ systematically reduces structural clustering of errors (lower SCS) for both classification
 421 (Figure 3(b)) and regression (Figure 3(d)) tasks. However, these improvements in structural uni-
 422 formity come at a slight cost to predictive accuracy, as demonstrated by decreased ACC scores for
 423 classification (Figure 3(a)) and increased MSE for regression (Figure 3(c)). Consequently, λ acts as
 424 a trade-off parameter balancing the structural uniformity of prediction errors against overall pre-
 425 dictive accuracy. Empirically, we identify $\lambda = 0.1$ as a favorable setting for our settings, achieving a
 426 substantial reduction in structural clustering without significantly compromising predictive per-
 427 formance, as summarized in Table 1.
 428

5 RELATED WORKS

430 Graph representation learning has received substantial attention recently, driven by the increasing
 431 necessity to effectively analyze complex relational structures embedded within graph data (see com-

432 prehensive surveys by Hamilton (2020); Kazemi et al. (2020)). Among various approaches, Graph
 433 Neural Networks (GNNs) have proven particularly effective, achieving state-of-the-art performance
 434 across diverse graph-related tasks, notably in spatial applications such as traffic forecasting, urban
 435 planning, and environmental monitoring (Jiang & Luo, 2022; Dong et al., 2023; Zhang et al., 2023).
 436 Broadly, existing GNN architectures can be categorized into three main classes based on their struc-
 437 tural learning approaches: (1) *message-passing methods*, which aggregate local neighborhood infor-
 438 mation to capture immediate graph connectivity (Kipf & Welling, 2017; Xu et al., 2020; Veličković
 439 et al., 2017); (2) *spectral-based methods*, leveraging graph Laplacian eigen-decompositions to en-
 440 code global structural information (Defferrard et al., 2016; Bruna et al., 2013); and (3) *graph trans-
 441 former models*, utilizing self-attention mechanisms to model long-range node interactions and de-
 442 pendencies (Dwivedi & Bresson, 2020). Given their practical significance, extensive research efforts
 443 have focused on theoretical foundations (Jegelka, 2022; Bronstein et al., 2021), architectural innova-
 444 tions (Wu et al., 2020), and computational optimizations for efficient training and inference of
 445 GNNs (Shao et al., 2024; Fey et al., 2021).

446 Despite these advancements, recent studies emphasize that inadequate evaluation methodologies re-
 447 main a crucial barrier hindering further progress in the GNN field (Bechler-Speicher et al., 2025;
 448 Shchur et al., 2018). Rigorous and reproducible evaluation frameworks have become recognized as
 449 essential components of trustworthy and robust machine learning research, directly impacting model
 450 selection and practical deployment (Zhang et al., 2021; Pineau et al., 2021). Benchmarking studies
 451 in graph representation learning have comprehensively evaluated GNN performance across diverse
 452 hyperparameter configurations and learning paradigms, highlighting that evaluation outcomes can
 453 differ significantly under inductive versus transductive settings, as well as various temporal scenar-
 454 ios (Dwivedi et al., 2023; Dong et al., 2024; Errica et al., 2019; Hu et al., 2020; Lv et al., 2021).
 455 Furthermore, a growing body of literature has extended these evaluations to temporal domains, as-
 456 sessing the effectiveness of temporal GNN models in dynamic graph settings (Junuthula et al., 2018;
 457 Haghani & Keyvanpour, 2019; Poursafaei et al., 2022; Huang et al., 2024; Su & Wu, 2025).

458 Nevertheless, a crucial yet underexplored area in current research is the evaluation metrics of GNNs,
 459 particularly regarding structural error distributions. This paper addresses this gap by proposing a
 460 novel evaluation metric explicitly designed to capture and quantify structural clustering patterns in
 461 GNN prediction errors, providing deeper insights for model assessment and deployment.

462 6 CONCLUDING DISCUSSION

464 **Conclusion.** In this paper, we investigated evaluation metrics tailored for GNNs. We identified
 465 key limitations of conventional exchangeable metrics—such as ACC and MSE—in capturing essen-
 466 tial structural error patterns, particularly the distinction between clustered and randomly dispersed
 467 prediction errors. To address these limitations, we proposed SCS, a novel structure-aware evalua-
 468 tion metric, explicitly designed to quantify structural clustering in prediction errors. Additionally,
 469 we introduced an extension of this metric, termed SCA learning, which serves as a regularizer to
 470 mitigate structurally clustered errors during GNN training. Our extensive empirical evaluation con-
 471 firmed that the proposed metric provides deeper insights into structural error distributions, effec-
 472 tively distinguishing among different structural error patterns and improving both model selection
 473 and robustness in network structured tasks.

474 **Limitations and Future Work.** An intriguing observation from our empirical study is the strong
 475 relationship between structural error patterns and underlying structural properties of graphs, such
 476 as degree distributions. This correlation likely emerges because GNN predictions inherently de-
 477 pend on the provided graph topology. Further research is needed to thoroughly investigate this
 478 phenomenon and elucidate the precise mechanisms through which graph structure influences GNN
 479 predictive behaviors. Additionally, while our current framework focuses on structural error clus-
 480 tering, incorporating temporal dynamics or other structural patterns into this evaluation approach
 481 represents a promising direction for future work. We provide an extended discussion of these poten-
 482 tial extensions in Appendix D.2. Integrating temporal dimensions would significantly enhance the
 483 applicability and robustness of our framework, enabling more comprehensive evaluations for GNNs
 484 in spatial-temporal contexts.

486
487
ETHICS STATEMENT488
489
490
491
492
493
494
495
496
497
498
499
500
501
502
503
504
505
506
507
508
509
510
511
512
513
514
515
516
517
518
519
520
521
522
523
524
525
526
527
528
529
530
531
532
533
534
535
536
537
538
539
540
541
542
543
544
545
546
547
548
549
550
551
552
553
554
555
556
557
558
559
560
561
562
563
564
565
566
567
568
569
570
571
572
573
574
575
576
577
578
579
580
581
582
583
584
585
586
587
588
589
590
591
592
593
594
595
596
597
598
599
600
601
602
603
604
605
606
607
608
609
610
611
612
613
614
615
616
617
618
619
620
621
622
623
624
625
626
627
628
629
630
631
632
633
634
635
636
637
638
639
640
641
642
643
644
645
646
647
648
649
650
651
652
653
654
655
656
657
658
659
660
661
662
663
664
665
666
667
668
669
670
671
672
673
674
675
676
677
678
679
680
681
682
683
684
685
686
687
688
689
690
691
692
693
694
695
696
697
698
699
700
701
702
703
704
705
706
707
708
709
710
711
712
713
714
715
716
717
718
719
720
721
722
723
724
725
726
727
728
729
730
731
732
733
734
735
736
737
738
739
740
741
742
743
744
745
746
747
748
749
750
751
752
753
754
755
756
757
758
759
759
760
761
762
763
764
765
766
767
768
769
770
771
772
773
774
775
776
777
778
779
779
780
781
782
783
784
785
786
787
788
789
789
790
791
792
793
794
795
796
797
798
799
800
801
802
803
804
805
806
807
808
809
809
810
811
812
813
814
815
816
817
818
819
819
820
821
822
823
824
825
826
827
828
829
829
830
831
832
833
834
835
836
837
838
839
839
840
841
842
843
844
845
846
847
848
849
849
850
851
852
853
854
855
856
857
858
859
859
860
861
862
863
864
865
866
867
868
869
869
870
871
872
873
874
875
876
877
878
879
879
880
881
882
883
884
885
886
887
888
889
889
890
891
892
893
894
895
896
897
898
899
900
901
902
903
904
905
906
907
908
909
909
910
911
912
913
914
915
916
917
918
919
919
920
921
922
923
924
925
926
927
928
929
929
930
931
932
933
934
935
936
937
938
939
939
940
941
942
943
944
945
946
947
948
949
949
950
951
952
953
954
955
956
957
958
959
959
960
961
962
963
964
965
966
967
968
969
969
970
971
972
973
974
975
976
977
978
979
979
980
981
982
983
984
985
986
987
988
989
989
990
991
992
993
994
995
996
997
998
999
1000
1001
1002
1003
1004
1005
1006
1007
1008
1009
1009
1010
1011
1012
1013
1014
1015
1016
1017
1018
1019
1019
1020
1021
1022
1023
1024
1025
1026
1027
1028
1029
1029
1030
1031
1032
1033
1034
1035
1036
1037
1038
1039
1039
1040
1041
1042
1043
1044
1045
1046
1047
1048
1049
1049
1050
1051
1052
1053
1054
1055
1056
1057
1058
1059
1059
1060
1061
1062
1063
1064
1065
1066
1067
1068
1069
1069
1070
1071
1072
1073
1074
1075
1076
1077
1078
1079
1079
1080
1081
1082
1083
1084
1085
1086
1087
1088
1089
1089
1090
1091
1092
1093
1094
1095
1096
1097
1098
1099
1099
1100
1101
1102
1103
1104
1105
1106
1107
1108
1109
1109
1110
1111
1112
1113
1114
1115
1116
1117
1118
1119
1119
1120
1121
1122
1123
1124
1125
1126
1127
1128
1129
1129
1130
1131
1132
1133
1134
1135
1136
1137
1138
1139
1139
1140
1141
1142
1143
1144
1145
1146
1147
1148
1149
1149
1150
1151
1152
1153
1154
1155
1156
1157
1158
1159
1159
1160
1161
1162
1163
1164
1165
1166
1167
1168
1169
1169
1170
1171
1172
1173
1174
1175
1176
1177
1178
1179
1179
1180
1181
1182
1183
1184
1185
1186
1187
1188
1189
1189
1190
1191
1192
1193
1194
1195
1196
1197
1198
1199
1199
1200
1201
1202
1203
1204
1205
1206
1207
1208
1209
1209
1210
1211
1212
1213
1214
1215
1216
1217
1218
1219
1219
1220
1221
1222
1223
1224
1225
1226
1227
1228
1229
1229
1230
1231
1232
1233
1234
1235
1236
1237
1238
1239
1239
1240
1241
1242
1243
1244
1245
1246
1247
1248
1249
1249
1250
1251
1252
1253
1254
1255
1256
1257
1258
1259
1259
1260
1261
1262
1263
1264
1265
1266
1267
1268
1269
1269
1270
1271
1272
1273
1274
1275
1276
1277
1278
1279
1279
1280
1281
1282
1283
1284
1285
1286
1287
1288
1289
1289
1290
1291
1292
1293
1294
1295
1296
1297
1298
1299
1299
1300
1301
1302
1303
1304
1305
1306
1307
1308
1309
1309
1310
1311
1312
1313
1314
1315
1316
1317
1318
1319
1319
1320
1321
1322
1323
1324
1325
1326
1327
1328
1329
1329
1330
1331
1332
1333
1334
1335
1336
1337
1338
1339
1339
1340
1341
1342
1343
1344
1345
1346
1347
1348
1349
1349
1350
1351
1352
1353
1354
1355
1356
1357
1358
1359
1359
1360
1361
1362
1363
1364
1365
1366
1367
1368
1369
1369
1370
1371
1372
1373
1374
1375
1376
1377
1378
1379
1379
1380
1381
1382
1383
1384
1385
1386
1387
1388
1389
1389
1390
1391
1392
1393
1394
1395
1396
1397
1398
1399
1399
1400
1401
1402
1403
1404
1405
1406
1407
1408
1409
1409
1410
1411
1412
1413
1414
1415
1416
1417
1418
1419
1419
1420
1421
1422
1423
1424
1425
1426
1427
1428
1429
1429
1430
1431
1432
1433
1434
1435
1436
1437
1438
1439
1439
1440
1441
1442
1443
1444
1445
1446
1447
1448
1449
1449
1450
1451
1452
1453
1454
1455
1456
1457
1458
1459
1459
1460
1461
1462
1463
1464
1465
1466
1467
1468
1469
1469
1470
1471
1472
1473
1474
1475
1476
1477
1478
1479
1479
1480
1481
1482
1483
1484
1485
1486
1487
1488
1489
1489
1490
1491
1492
1493
1494
1495
1496
1497
1498
1499
1499
1500
1501
1502
1503
1504
1505
1506
1507
1508
1509
1509
1510
1511
1512
1513
1514
1515
1516
1517
1518
1519
1519
1520
1521
1522
1523
1524
1525
1526
1527
1528
1529
1529
1530
1531
1532
1533
1534
1535
1536
1537
1538
1539
1539
1540
1541
1542
1543
1544
1545
1546
1547
1548
1549
1549
1550
1551
1552
1553
1554
1555
1556
1557
1558
1559
1559
1560
1561
1562
1563
1564
1565
1566
1567
1568
1569
1569
1570
1571
1572
1573
1574
1575
1576
1577
1578
1579
1579
1580
1581
1582
1583
1584
1585
1586
1587
1588
1589
1589
1590
1591
1592
1593
1594
1595
1596
1597
1598
1599
1599
1600
1601
1602
1603
1604
1605
1606
1607
1608
1609
1609
1610
1611
1612
1613
1614
1615
1616
1617
1618
1619
1619
1620
1621
1622
1623
1624
1625
1626
1627
1628
1629
1629
1630
1631
1632
1633
1634
1635
1636
1637
1638
1639
1639
1640
1641
1642
1643
1644
1645
1646
1647
1648
1649
1649
1650
1651
1652
1653
1654
1655
1656
1657
1658
1659
1659
1660
1661
1662
1663
1664
1665
1666
1667
1668
1669
1669
1670
1671
1672
1673
1674
1675
1676
1677
1678
1679
1679
1680
1681
1682
1683
1684
1685
1686
1687
1688
1689
1689
1690
1691
1692
1693
1694
1695
1696
1697
1698
1699
1699
1700
1701
1702
1703
1704
1705
1706
1707
1708
1709
1709
1710
1711
1712
1713
1714
1715
1716
1717
1718
1719
1719
1720
1721
1722
1723
1724
1725
1726
1727
1728
1729
1729
1730
1731
1732
1733
1734
1735
1736
1737
1738
1739
1739
1740
1741
1742
1743
1744
1745
1746
1747
1748
1749
1749
1750
1751
1752
1753
1754
1755
1756
1757
1758
1759
1759
1760
1761
1762
1763
1764
1765
1766
1767
1768
1769
1769
1770
1771
1772
1773
1774
1775
1776
1777
1778
1779
1779
1780
1781
1782
1783
1784
1785
1786
1787
1788
1789
1789
1790
1791
1792
1793
1794
1795
1796
1797
1798
1799
1799
1800
1801
1802
1803
1804
1805
1806
1807
1808
1809
1809
1810
1811
1812
1813
1814
1815
1816
1817
1818
1819
1819
1820
1821
1822
1823
1824
1825
1826
1827
1828
1829
1829
1830
1831
1832
1833
1834
1835
1836
1837
1838
1839
1839
1840
1841
1842
1843
1844
1845
1846
1847
1848
1849
1849
1850
1851
1852
1853
1854
1855
1856
1857
1858
1859
1859
1860
1861
1862
1863
1864
1865
1866
1867
1868
1869
1869
1870
1871
1872
1873
1874
1875
1876
1877
1878
1879
1879
1880
1881
1882
1883
1884
1885
1886
1887
1888
1889
1889
1890
1891
1892
1893
1894
1895
1896
1897
1898
1899
1899
1900
1901
1902
1903
1904
1905
1906
1907
1908
1909
1909
1910
1911
1912
1913
1914
1915
1916
1917
1918
1919
1919
1920
1921
1922
1923
1924
1925
1926
1927
1928
1929
1929
1930
1931
1932
1933
1934
1935
1936
1937
1938
1939
1939
1940
1941
1942
1943
1944
1945
1946
1947
1948
1949
1949
1950
1951
1952
1953
1954
1955
1956
1957
1958
1959
1959
1960
1961
1962
1963
1964
1965
1966
1967
1968
1969
1969
1970
1971
1972
1973
1974
1975
1976
1977
1978
1979
1979
1980
1981
1982
1983
1984
1985
1986
1987
1988
1989
1989
1990
1991
1992
1993
1994
1995
1996
1997
1998
1999
1999
2000
2001
2002
2003
2004
2005
2006
2007
2008
2009
2009
2010
2011
2012
2013
2014
2015
2016
2017
2018
2019
2019
2020
2021
2022
2023
2024
2025
2026
2027
2028
2029
2029
2030
2031
2032
2033
2034
2035
2036
2037
2038
2039
2039
2040
2041
2042
2043
2044
2045
2046
2047
2048
2049
2049
2050
2051
2052
2053
2054
2055
2056
2057
2058
2059
2059
2060
2061
2062
2063
2064
2065
2066
2067
2068
2069
2069
2070
2071
2072
2073
2074
2075
2076
2077
2078
2079
2079
2080
2081
2082
2083
2084
2085
2086
2087
2088
2089
2089
2090
2091
2092
2093
2094
2095
2096
2097
2098
2099
2099
2100
2101
2102
2103
2104
2105
2106
2107
2108
2109
2109
2110
2111
2112
2113
2114
2115
2116
2117
2118
2119
2119
2120
2121
2122
2123
2124
2125
2126
2127
2128
2129
2129
2130
2131
2132
2133
2134
2135
2136
2137
2138
2139
2139
2140
2141
2142
2143
2144
2145
2146
2147
2148
2149
2149
2150
2151
2152
2153
2154
2155
2156
2157
2158
2159
2159
2160
2161
2162
2163
2164
2165
2166
2167
2168
2169
2169
2170
2171
2172
2173
2174
2175
2176
2177
2178
2179
2179
2180
2181
2182
2183
2184
2185
2186
2187
2188
2189
2189
2190
2191
2192
2193
2194
2195
2196
2197
2198
2199
2199
2200
2201
2202
2203
2204
2205
2206
2207
2208
2209
2209
2210
2211
2212
2213
2214
2215
2216
2217
2218
2219
2219
2220
2221
2222
2223
2224
2225
2226
2227
2228
2229
2229
2230
2231
2232
2233
2234
2235
2236
2237
2238
2239
2239
2240
2241
2242
2243
2244
2245
2246
2247
2248
2249
2249
2250
2251
2252
2253
2254
2255
2256
2257
2258
2259
2259
2260
2261
2262
2263
2264
2265
2266
2267
2268
2269
2269
2270
2271
2272
2273
2274
2275
2276
2277
2278
2279
2279
2280
2281
2282
2283
2284
2285
2286
2287
2288
2289
2289
2290
2291
2292
2293
2294
2295
2296
2297
2298
2299
2299
2300
2301
2302
2303
2304<br

540 Muhammad Farhan Fathurrahman and Sidharta Gautama. Spatial performance indicators to evaluate
 541 spatiotemporal traffic prediction. In *VEHITS*, pp. 156–164, 2024.

542

543 Matthias Fey, Jan E Lenssen, Frank Weichert, and Jure Leskovec. Gnnautoscale: Scalable and
 544 expressive graph neural networks via historical embeddings. In *International Conference on
 545 Machine Learning*, pp. 3294–3304. PMLR, 2021.

546 Shengnan Guo, Youfang Lin, Ning Feng, Chao Song, and Huaiyu Wan. Attention based spatial-
 547 temporal graph convolutional networks for traffic flow forecasting. In *Proceedings of the AAAI
 548 conference on artificial intelligence*, volume 33, pp. 922–929, 2019.

549 Sogol Haghani and Mohammad Reza Keyvanpour. A systemic analysis of link prediction in social
 550 network. *Artificial Intelligence Review*, 52:1961–1995, 2019.

551

552 Will Hamilton, Zhitao Ying, and Jure Leskovec. Inductive representation learning on large graphs.
 553 *Advances in neural information processing systems*, 30, 2017.

554 William L Hamilton. Graph representation learning. *Synthesis Lectures on Artificial Intelligence and
 555 Machine Learning*, 14(3):1–159, 2020.

556

557 J Hooker, G Duveiller, and A Cescatti. A global dataset of air temperature derived from satellite
 558 remote sensing and weather stations. *sci. data*, 5, 180246, 2018.

559 Weihua Hu, Matthias Fey, Marinka Zitnik, Yuxiao Dong, Hongyu Ren, Bowen Liu, Michele Catasta,
 560 and Jure Leskovec. Open graph benchmark: Datasets for machine learning on graphs. *Advances
 561 in neural information processing systems*, 33:22118–22133, 2020.

562

563 Qian Huang, Horace He, Abhay Singh, Ser-Nam Lim, and Austin Benson. Combining label prop-
 564 agation and simple models out-performs graph neural networks. In *International Conference on
 565 Learning Representations*.

566

567 Shenyang Huang, Farimah Poursafaei, Jacob Danovitch, Matthias Fey, Weihua Hu, Emanuele Rossi,
 568 Jure Leskovec, Michael Bronstein, Guillaume Rabusseau, and Reihaneh Rabbany. Temporal
 569 graph benchmark for machine learning on temporal graphs. *Advances in Neural Information
 Processing Systems*, 36, 2024.

570

571 Stefanie Jegelka. Theory of graph neural networks: Representation and learning, 2022. URL
<https://arxiv.org/abs/2204.07697>.

572

573 Weiwei Jiang and Jiayun Luo. Graph neural network for traffic forecasting: A survey. *Expert
 574 Systems with Applications*, 207:117921, November 2022. ISSN 0957-4174. doi: 10.1016/j.eswa.
 575 2022.117921. URL <http://dx.doi.org/10.1016/j.eswa.2022.117921>.

576

577 Ruthwik Junuthula, Kevin Xu, and Vijay Devabhaktuni. Leveraging friendship networks for dy-
 578 namic link prediction in social interaction networks. In *Proceedings of the International AAAI
 579 Conference on Web and Social Media*, volume 12, 2018.

580

581 Seyed Mehran Kazemi, Rishab Goel, Kshitij Jain, Ivan Kobyzev, Akshay Sethi, Peter Forsyth, and
 582 Pascal Poupart. Representation learning for dynamic graphs: A survey. *The Journal of Machine
 583 Learning Research*, 21(1):2648–2720, 2020.

584

585 Thomas N. Kipf and Max Welling. Semi-supervised classification with graph convolutional net-
 586 works, 2017.

587

588 Yanhua Li, Xun Zhou, and Menghai Pan. Graph neural networks in urban intelligence. *Graph
 589 Neural Networks: Foundations, Frontiers, and Applications*, pp. 579–593, 2022.

590

591 Zilin Li, Haixing Liu, Chi Zhang, and Guangtao Fu. Real-time water quality prediction in water
 592 distribution networks using graph neural networks with sparse monitoring data. *Water Research*,
 593 250:121018, 2024.

594

595 Qingsong Lv, Ming Ding, Qiang Liu, Yuxiang Chen, Wenzheng Feng, Siming He, Chang Zhou,
 596 Jianguo Jiang, Yuxiao Dong, and Jie Tang. Are we really making much progress? revisiting,
 597 benchmarking and refining heterogeneous graph neural networks. In *Proceedings of the 27th
 598 ACM SIGKDD conference on knowledge discovery & data mining*, pp. 1150–1160, 2021.

594 Patrick AP Moran. Notes on continuous stochastic phenomena. *Biometrika*, 37(1/2):17–23, 1950.
 595

596 Davide Moretti, Elia Onofri, and Emiliano Cristiani. Detection of anomalous vehicular traffic and
 597 sensor failures using data clustering techniques. *arXiv preprint arXiv:2504.00881*, 2025.

598 R Kelley Pace and Ronald Barry. Sparse spatial autoregressions. *Statistics & Probability Letters*, 33
 599 (3):291–297, 1997.

600

601 Joelle Pineau, Philippe Vincent-Lamarre, Koustuv Sinha, Vincent Larivière, Alina Beygelzimer,
 602 Florence d’Alché Buc, Emily Fox, and Hugo Larochelle. Improving reproducibility in machine
 603 learning research (a report from the neurips 2019 reproducibility program). *Journal of machine
 604 learning research*, 22(164):1–20, 2021.

605 Farimah Poursafaei, Shenyang Huang, Kellin Peltz, , and Reihaneh Rabbany. Towards better
 606 evaluation for dynamic link prediction. In *Neural Information Processing Systems (NeurIPS)
 607 Datasets and Benchmarks*, 2022.

608 Morteza Saadati, Sayyed Majid Mazinani, Ali Akbar Khazaei, and Seyyed Javad Seyyed Mahdavi
 609 Chabok. Energy efficient clustering for dense wireless sensor network by applying graph neural
 610 networks with coverage metrics. *Ad Hoc Networks*, 156:103432, 2024.

611

612 Prithviraj Sen, Galileo Namata, Mustafa Bilgic, Lise Getoor, Brian Gallagher, and Tina Eliassi-Rad.
 613 Collective classification in network data. *AI Magazine*, 29(3):93–106, 2008.

614 Yingxia Shao, Hongzheng Li, Xizhi Gu, Hongbo Yin, Yawen Li, Xupeng Miao, Wentao Zhang,
 615 Bin Cui, and Lei Chen. Distributed graph neural network training: A survey. *ACM Computing
 616 Surveys*, 56(8):1–39, 2024.

617 Oleksandr Shchur, Maximilian Mumme, Aleksandar Bojchevski, and Stephan Günnemann. Pitfalls
 618 of graph neural network evaluation. *arXiv preprint arXiv:1811.05868*, 2018.

619

620 Junwei Su and Shan Wu. Temporal-aware evaluation and learning for temporal graph neural net-
 621 works. In *Proceedings of the AAAI Conference on Artificial Intelligence*, volume 39, pp. 20628–
 622 20636, 2025.

623 Petar Veličković, Guillem Cucurull, Arantxa Casanova, Adriana Romero, Pietro Lio, and Yoshua
 624 Bengio. Graph attention networks. *arXiv preprint arXiv:1710.10903*, 2017.

625

626 Zonghan Wu, Shirui Pan, Fengwen Chen, Guodong Long, Chengqi Zhang, and S Yu Philip. A
 627 comprehensive survey on graph neural networks. *IEEE transactions on neural networks and
 628 learning systems*, 32(1):4–24, 2020.

629 Chuan Xu, Jingqin Gao, Fan Zuo, and Kaan Ozbay. Estimating urban traffic safety and analyzing
 630 spatial patterns through the integration of city-wide near-miss data: A new york city case study.
 631 *Applied Sciences (2076-3417)*, 14(14), 2024.

632

633 Da Xu, Chuanwei Ruan, Evren Korpeoglu, Sushant Kumar, and Kannan Achan. Inductive represen-
 634 tation learning on temporal graphs. *arXiv preprint arXiv:2002.07962*, 2020.

635

636 Chiyuan Zhang, Samy Bengio, Moritz Hardt, Benjamin Recht, and Oriol Vinyals. Understanding
 637 deep learning (still) requires rethinking generalization. *Communications of the ACM*, 64(3):107–
 115, 2021.

638

639 Jing Zhang, Fu Xiao, Ao Li, Tianyou Ma, Kan Xu, Hanbei Zhang, Rui Yan, Xing Fang, Yuanyang
 640 Li, and Dan Wang. Graph neural network-based spatio-temporal indoor environment prediction
 641 and optimal control for central air-conditioning systems. *Building and Environment*, 242:110600,
 2023.

642

643 Qi Zhang, Jianlong Chang, Gaofeng Meng, Shiming Xiang, and Chunhong Pan. Spatio-temporal
 644 graph structure learning for traffic forecasting. In *Proceedings of the AAAI conference on artificial
 645 intelligence*, volume 34, pp. 1177–1185, 2020.

646

647 Ling Zhao, Yujiao Song, Chao Zhang, Yu Liu, Pu Wang, Tao Lin, Min Deng, and Haifeng Li. T-gcn:
 648 A temporal graph convolutional network for traffic prediction. *IEEE transactions on intelligent
 649 transportation systems*, 21(9):3848–3858, 2019a.

648 Xuzhi Zhao, Yahui Peng, Xian-gang Wang, Libing Zhu, and Houjin Chen. spatial uniformity as-
649 sessment of particles distributed in a spherical fuel element using a non-destructive approach.
650 *Scientific Reports*, 9(1):7885, 2019b.
651
652
653
654
655
656
657
658
659
660
661
662
663
664
665
666
667
668
669
670
671
672
673
674
675
676
677
678
679
680
681
682
683
684
685
686
687
688
689
690
691
692
693
694
695
696
697
698
699
700
701

702 THE USE OF LARGE LANGUAGE MODELS (LLMs)
703704 We used LLMs only as a general-purpose writing assistant to aid in grammar checking and polishing
705 the writing. The LLM did not contribute to research ideas, experiment design, theoretical analysis,
706 or result interpretation.
707708 A DIFFERENT GRAPH NEURAL NETWORKS FAMILIES
709710 Graph Neural Networks (GNNs) have become one of the most effective machine learning methods
711 for modeling relational and spatial data due to their powerful ability to encode complex structural
712 dependencies. Based on the approach used to capture graph dependencies, GNN architectures can
713 broadly be categorized into three main families: *spatial-based (message-passing) GNNs*, *spectral-
714 based GNNs*, and *graph transformers*. In this section, we provide a comprehensive introduction to
715 each of these GNN families, highlighting their theoretical foundations, advantages, and practical
716 considerations.
717718 A.1 SPATIAL-BASED (MESSAGE-PASSING) GNNs
719720 Spatial-based GNNs, also known as message-passing GNNs, operate directly on the graph structure
721 by iteratively aggregating and updating node representations based on their local neighborhoods.
722 Unlike spectral methods, they do not require eigen-decomposition of graph matrices, making them
723 computationally efficient and highly scalable for large graphs.
724724 Formally, the general message-passing paradigm for updating the embedding of node v at layer t
725 can be expressed as:
726

727
$$\mathbf{h}_v^{(t)} = \text{UPDATE}^{(t)} \left(\mathbf{h}_v^{(t-1)}, \text{AGGREGATE}^{(t)} \left(\{\mathbf{h}_u^{(t-1)} : u \in \mathcal{N}(v)\} \right) \right), \quad (\text{A.1})$$

728

729 where $\mathbf{h}_v^{(t)}$ is the embedding of node v at layer t , and $\mathcal{N}(v)$ denotes its immediate neighbors. Rep-
730 resentative models in this category include Graph Convolutional Networks (GCN) (Kipf & Welling,
731 2017), GraphSAGE (Hamilton et al., 2017), and Graph Attention Networks (GAT) (Veličković et al.,
732 2017). Spatial-based GNNs naturally encode local structural information and gradually capture
733 broader structural context as the network depth increases. However, excessively deep message-
734 passing architectures often suffer from oversmoothing, where node representations converge, reduc-
735 ing their discriminative power.
736

737 A.2 SPECTRAL-BASED GNNs

738 Spectral-based GNNs leverage graph spectral theory and define graph convolutions using spectral
739 filtering based on eigen-decomposition of the graph Laplacian. Specifically, given the normalized
740 Laplacian matrix $\hat{\mathbf{L}} = \mathbf{U}\Lambda\mathbf{U}^\top$, where \mathbf{U} represents eigenvectors and Λ is a diagonal matrix of
741 eigenvalues, the spectral convolution operation on node features \mathbf{x} with a parameterized filter $g_\theta(\cdot)$
742 is defined as:
743

744
$$\mathbf{x} * \mathbf{g}_\theta = \mathbf{U}g_\theta(\Lambda)\mathbf{U}^\top \mathbf{x}. \quad (\text{A.2})$$

745 Early spectral-based GNNs explicitly computed the eigen-decomposition, leading to significant
746 computational complexity. To address this limitation, practical implementations such as Chebyshev
747 networks (ChebNet) (Defferrard et al., 2016) and the simplified Graph Convolutional Networks by
748 Kipf & Welling (2017) use polynomial approximations, significantly enhancing computational
749 efficiency. While spectral-based methods effectively capture global structural properties of graphs,
750 their reliance on spectral decomposition makes them inherently less scalable for large-scale graph
751 datasets compared to spatial-based approaches.
752

753 A.3 GRAPH TRANSFORMERS

754 Graph transformers extend the spatial-based message-passing framework by incorporating self-
755 attention mechanisms, allowing models to adaptively weigh information from nodes across varying
756 distances within the graph. Inspired by transformer architectures initially developed for natural
757

756 language processing, graph transformers apply attention mechanisms directly to graph structures to
 757 capture both local and long-range dependencies.
 758

759 Formally, given node embeddings \mathbf{h}_v and \mathbf{h}_u , the attention mechanism computes attention coefficients
 760 α_{vu} between nodes v and u as follows:

$$\alpha_{vu} = \frac{\exp(\text{Attn}(\mathbf{h}_v, \mathbf{h}_u))}{\sum_{k \in \mathcal{V}} \exp(\text{Attn}(\mathbf{h}_v, \mathbf{h}_k))}, \quad (\text{A.3})$$

761 where \mathcal{V} represents the set of nodes. Unlike traditional message-passing approaches, graph trans-
 762 formers can dynamically and selectively attend to neighbors at varying graph distances, making
 763 them highly effective in modeling complex spatial interactions. To incorporate structural informa-
 764 tion explicitly, graph transformers typically use positional encodings derived from the graph struc-
 765 ture, thereby augmenting node feature representations. Despite their ability to capture richer rep-
 766 resentations and dependencies, graph transformers typically require more computational resources,
 767 especially for larger graphs, due to the quadratic complexity associated with computing pairwise
 768 attention scores.
 769

771 A.4 COMPARISON AND MOTIVATION

772 Empirical comparisons among spatial-based GNNs, spectral-based GNNs, and graph trans-
 773 formers often indicate similar overall predictive performances (measured by metrics like accuracy) across
 774 various datasets. The primary differences between these families generally manifest in their trade-
 775 offs regarding computational efficiency and the scope of structural information captured. Specifi-
 776 cally, spatial-based methods offer scalability and efficient local aggregation but may have difficulty
 777 encoding global structures effectively without increased depth. Spectral-based methods explicitly
 778 encode global structure but can be computationally prohibitive for large-scale graphs. Graph trans-
 779 formers flexibly capture both local and global dependencies but at a higher computational cost.
 780

781 The subtle performance differences and limited understanding of each family’s capability to capture
 782 specific graph structures underscore the importance of systematically evaluating and understanding
 783 GNN models. This necessity motivates our work in this paper—focusing on the development of
 784 spatially-aware evaluation metrics capable of revealing nuanced differences in GNN performance,
 785 particularly in spatial applications.
 786

787 B PROOFS

788 In this appendix, we present a proof for Theorem 3.1.

789 **Proof of Theorem 3.1.** Recall from Definition 2 that an evaluation metric $\mu(\cdot)$ is exchangeable if,
 790 for any permutation π of node indices, the metric satisfies:

$$791 \mu(\epsilon) = \mu(\pi(\epsilon)).$$

792 Let \mathbb{P}_1 and \mathbb{P}_2 be two distinct error distributions for a given GNN applied to a graph $\mathcal{G} = (\mathcal{V}, \mathcal{E})$,
 793 where $|\mathcal{V}| = N$. Suppose additionally:

$$794 \mathbb{E}_{\mathbb{P}_1} [S(\epsilon)] = \mathbb{E}_{\mathbb{P}_2} [S(\epsilon)],$$

795 where the sum-based metric is defined as:
 796

$$800 S(\epsilon) = \sum_{v \in \mathcal{V}} f(y_v, \hat{y}_v).$$

801 Since $\mu(\cdot)$ is exchangeable, its evaluation depends solely on the multiset of error values
 802 $\{\epsilon_1, \epsilon_2, \dots, \epsilon_N\}$ rather than on their spatial arrangement or indexing.
 803

804 Notice that the metric $S(\epsilon)$ itself is inherently exchangeable, as it is simply a sum over nodes,
 805 invariant under permutations. Thus, the condition:
 806

$$807 \mathbb{E}_{\mathbb{P}_1} [S(\epsilon)] = \mathbb{E}_{\mathbb{P}_2} [S(\epsilon)]$$

808 implies that the two distributions \mathbb{P}_1 and \mathbb{P}_2 yield identical expectations for every exchangeable
 809 aggregation of errors, as these aggregations remain invariant under any permutation.
 810

810 Let \mathcal{E}_m denote the set of all possible multisets of error values. Since $\mu(\cdot)$ is exchangeable, we can
 811 express its expectation under a given distribution \mathbb{P} as:

$$812 \quad 813 \quad 814 \quad \mathbb{E}_{\mathbb{P}}[\mu(\epsilon)] = \sum_{E \in \mathcal{E}_m} \mu(E) \mathbb{P}(E),$$

815 where $\mathbb{P}(E)$ represents the probability of observing the error multiset E .

816 Given the earlier equality for the sum-based aggregation, we have:

$$817 \quad 818 \quad 819 \quad \mathbb{E}_{\mathbb{P}_1}[S(\epsilon)] = \sum_{E \in \mathcal{E}_m} S(E) \mathbb{P}_1(E) = \sum_{E \in \mathcal{E}_m} S(E) \mathbb{P}_2(E) = \mathbb{E}_{\mathbb{P}_2}[S(\epsilon)].$$

820 Because this equality holds for every exchangeable sum-based aggregation $S(E)$, it follows directly
 821 that for each multiset E , we must have:

$$822 \quad 823 \quad \mathbb{P}_1(E) = \mathbb{P}_2(E), \quad \forall E \in \mathcal{E}_m.$$

824 Therefore, since the evaluation metric $\mu(\cdot)$ is solely dependent on these multisets (due to exchange-
 825 ability), we obtain:

$$826 \quad 827 \quad 828 \quad \mathbb{E}_{\mathbb{P}_1}[\mu(\epsilon)] = \sum_{E \in \mathcal{E}_m} \mu(E) \mathbb{P}_1(E) = \sum_{E \in \mathcal{E}_m} \mu(E) \mathbb{P}_2(E) = \mathbb{E}_{\mathbb{P}_2}[\mu(\epsilon)].$$

830 Hence, we have formally shown that if two error distributions yield identical expectations for ex-
 831 changeable sum-based aggregations, any exchangeable evaluation metric will fail to differentiate
 832 between these distributions. Thus, we establish the theorem statement:

$$833 \quad \mathbb{E}_{\mathbb{P}_1}[\mu(\epsilon)] = \mathbb{E}_{\mathbb{P}_2}[\mu(\epsilon)],$$

834 as required. □

835 B.1 LIMITATIONS OF SHORTEST-PATH DISTANCE AND ADVANTAGES OF SCS

836 Accurately evaluating spatial prediction errors in graph neural networks (GNNs) demands metrics
 837 that explicitly consider spatial relationships among nodes. Although an intuitive spatial measure
 838 might employ the average shortest-path distance between incorrectly predicted nodes, this naive
 839 metric faces significant practical and interpretative limitations. Consequently, we propose the Spatial
 840 Cluster Statistic (SCS), a robust metric that effectively captures spatial clustering by measuring
 841 spatial autocorrelation among prediction errors.

842 **Failure of Shortest-Path Distance Metrics.** A straightforward spatial evaluation approach in-
 843 volves computing the average shortest-path distance between nodes where prediction errors occur.
 844 At first glance, this method seems effective: smaller average distances might indicate spatially clus-
 845 tered errors, whereas larger average distances could reflect more dispersed errors. However, this
 846 approach exhibits several fundamental flaws:

- 847 • **Computational Complexity:** Shortest-path computations generally incur high compu-
 848 tational costs, scaling poorly with network size. Typical algorithms such as Floyd-
 849 Warshall or multiple runs of Dijkstra’s algorithm have time complexities of $O(N^3)$ and
 850 $O(N^2 \log N)$, respectively, making them impractical for large spatial networks or frequent
 851 evaluations ?.
- 852 • **Distortion by Graph Structure:** In many real-world networks characterized by irregular
 853 connectivity or hub-like structures (such as scale-free graphs), shortest-path metrics are
 854 disproportionately influenced by high-degree nodes (hubs). Errors connected through hubs
 855 may exhibit artificially small distances despite being geographically distant, obscuring gen-
 856 uine spatial clustering patterns and limiting the interpretability of results Barabási (2013).
- 857 • **Ambiguity in Spatial Interpretation:** Shortest-path distances in graphs do not directly
 858 correspond to true spatial or geographical distances. Consequently, interpreting spatial pat-
 859 terns based solely on shortest-path measures can be misleading. Nodes that are physically
 860 far apart might have short graph distances due to high connectivity, while physically adja-
 861 cent nodes could have long shortest-path distances if connections are sparse or irregular.

864
 865
 866
 867
 868
 869
 870 • **Inability to Identify Genuine Clustering:** Shortest-path metrics fail to distinguish
 871 between spatially meaningful clusters of errors and coincidental proximity caused by graph
 872 topology. Such metrics focus exclusively on distance magnitude, overlooking the crucial
 873 spatial autocorrelation (the correlation of errors between neighboring nodes), essential for
 874 identifying systematic spatial patterns.

875 Due to these critical limitations, shortest-path-based metrics are fundamentally inadequate for rig-
 876 orously capturing spatial clustering in GNN prediction errors.

877 **Advantages and Interpretation of SCS.** To address these limitations, we introduce the Spatial
 878 Cluster Statistic (SCS), inspired by Moran’s I statistic from spatial statistics. SCS explicitly accounts
 879 for spatial autocorrelation, quantifying how prediction errors at each node correlate with errors at
 880 neighboring nodes. Formally, given the prediction errors $\epsilon_v = f(y_v, \hat{y}_v)$ for each node v in a test set
 881 $\mathcal{V}_{\text{test}}$, SCS is defined as:

$$882 \quad 883 \quad 884 \quad 885 \quad 886 \quad 887 \quad 888 \quad 889 \quad 890 \quad 891 \quad 892 \quad 893 \quad 894 \quad 895 \quad 896 \quad 897 \quad 898 \quad 899 \quad 900 \quad 901 \quad 902 \quad 903 \quad 904 \quad 905 \quad 906 \quad 907 \quad 908 \quad 909 \quad 910 \quad 911 \quad 912 \quad 913 \quad 914 \quad 915 \quad 916 \quad 917 \quad \text{SCS}(\epsilon, \mathcal{V}_{\text{test}}) = \frac{k}{W} \frac{\sum_{v,u \in \mathcal{V}_{\text{test}}} w_{vu}(\epsilon_v - \bar{\epsilon})(\epsilon_u - \bar{\epsilon})}{\sum_{v \in \mathcal{V}_{\text{test}}} (\epsilon_v - \bar{\epsilon})^2}, \quad (\text{B.1})$$

where:

- $\bar{\epsilon} = \frac{1}{k} \sum_{v \in \mathcal{V}_{\text{test}}} \epsilon_v$ is the mean error across test nodes;
- w_{vu} are spatial weights, typically adjacency-based ($w_{vu} = 1$ if nodes v and u are neigh-
 885 bors, otherwise 0);
- $W = \sum_{v,u \in \mathcal{V}_{\text{test}}} w_{vu}$ represents the total weight sum;
- $k = |\mathcal{V}_{\text{test}}|$ is the number of test nodes.

SCS possesses several important advantages and clear interpretative properties:

891
 892 • **Explicit Spatial Autocorrelation Measurement:** Unlike shortest-path metrics, SCS di-
 893 rectly quantifies the spatial correlation of errors among neighboring nodes. Positive SCS
 894 values indicate pronounced spatial clustering of errors, revealing localized model inac-
 895 curacies. Conversely, negative values highlight dispersed error patterns, indicating that errors
 896 occur in a spatially repulsive manner.

897 • **Robustness to Graph Topology:** Because SCS evaluates autocorrelation based explic-
 898 itely on neighborhood structures rather than shortest paths, it is inherently more robust to
 899 irregular graph structures and less distorted by highly connected nodes or hubs.

900 • **Computational Efficiency:** SCS computation is highly efficient and scalable ($O(E)$) com-
 901 plexity, where E is the number of edges in the test subgraph), making it practical for re-
 902 peated evaluation, hyperparameter tuning, and real-time monitoring of model performance
 903 on large-scale spatial networks.

904 • **Interpretability and Practical Insights:** SCS provides meaningful, actionable insights
 905 into spatial error structures. High positive values clearly indicate specific regions or node
 906 clusters needing model improvement or immediate attention, significantly enhancing inter-
 907 pretability and practical decision-making capabilities.

908 In summary, while shortest-path-based measures fail due to computational, structural, and inter-
 909 pretative issues, the proposed SCS provides a robust, interpretable, and efficient metric explicitly
 910 designed to capture spatial clustering patterns in GNN prediction errors. By clearly identifying spa-
 911 tially localized inaccuracies, SCS facilitates targeted interventions, model improvements, and robust
 912 deployments of GNN models in spatial applications.

C ADDITIONAL DETAILS ON EXPERIMENTS

913 In this appendix, we provide comprehensive details regarding the experimental setup, including
 914 datasets and tasks, baseline models, and training procedures, ensuring reproducibility and clarity.

918 C.1 TESTBED
919920 Our experiments were conducted on a Dell PowerEdge C4140, The key specifications of this server,
921 pertinent to our research, include:922 **CPU:** Dual Intel Xeon Gold 6230 processors, each offering 20 cores and 40 threads.923 **GPU:** Four NVIDIA Tesla V100 SXM2 units, each equipped with 32GB of memory, tailored for
924 NV Link.925 **Memory:** An aggregate of 256GB RAM, distributed across eight 32GB RDIMM modules.926 **Storage:** Dual 1.92TB SSDs with a 6Gbps SATA interface.927 **Networking:** Features dual 1Gbps NICs and a Mellanox ConnectX-5 EX Dual Port 40/100GbE
928 QSFP28 Adapter with GPUDirect support.929 **Operating System:** Ubuntu 18.04 LTS.930 We employed benchmark datasets that encompass node classification and node regression tasks to
931 comprehensively assess our method across diverse spatial contexts. Specifically:932 **Node Classification Datasets:**933

- **Cora**(Sen et al., 2008): A citation network with 2,708 nodes representing scientific papers
934 classified into 7 research categories. It has 5,429 citation links and sparse bag-of-words
935 node features (dimension: 1,433).
- **Citeseer**(Sen et al., 2008): Another widely adopted citation network with 3,327 nodes and
936 4,732 edges. Papers are classified into 6 research categories, with node features represented
937 by a 3,703-dimensional sparse bag-of-words.

938 **Node Regression Datasets:**939

- **California Housing Prices**(Pace & Barry, 1997): A spatial regression dataset with 20,640
940 nodes representing geographic locations in California. The goal is to predict the median
941 house prices based on spatial coordinates and associated features such as average income,
942 population density, and proximity to various infrastructure.
- **Air Temperature Dataset**(Hooker et al., 2018): Contains temperature measurements from
943 1,305 meteorological stations globally, aiming to predict average air temperature based on
944 geographical coordinates and associated climate factors.

945 **Synthetic Planar Datasets:** We synthesized two types of planar graphs to systematically analyze
946 the impact of underlying graph structures on spatial error patterns:947

- **Planar-Regular:** A uniformly connected planar graph generated with a regular node-
948 degree distribution, consisting of nodes arranged in a grid-like spatial structure.
- **Planar-Power-Law:** A planar graph with power-law degree distribution (scale-free prop-
949 erties). The synthetic generation procedure followed Barabási–Albert preferential attach-
950 ment (Barabási, 2013), modified to ensure planarity.

951 For all datasets, we either follow the default split (where provided) or followed standard data splits
952 with ratios of 60% for training, 20% for validation, and 20% for testing. Results were averaged
953 across five independent trials to ensure robustness and reproducibility.954 C.2 BASELINES
955956 We evaluated five representative baseline GNN architectures from three distinct methodological
957 categories to comprehensively benchmark our proposed methods:958 **Message-Passing GNNs:**959

- **GCN**(Kipf & Welling, 2017): Graph Convolutional Network employing normalized
960 adjacency-based feature aggregation.
- **GraphSAGE**(Hamilton et al., 2017): Aggregates features using neighborhood sampling
961 and mean-pooling.

972
973
974

- **GAT** (Veličković et al., 2017): Graph Attention Network employing self-attention mechanisms to weigh neighboring nodes.

975
976

Spectral-based GNN:

977
978
979

- **ChebNet** (Defferrard et al., 2016): Spectral convolution network approximating filters via Chebyshev polynomial expansions of the graph Laplacian.

980
981

Transformer-based GNN:

982
983
984

- **Graph Transformer** (Dwivedi & Bresson, 2020): Leverages global self-attention mechanisms to capture long-range node dependencies without explicit reliance on local message-passing.

985
986
987
988
989
990
991
992
993
994
995
996
997
998
999
1000
1001
1002
1003
1004
1005
1006
1007
1008
1009
1010
1011
1012
1013
1014
1015
1016
1017
1018
1019
1020
1021
1022
1023
1024
1025

We utilized standard open-source implementations from widely adopted libraries (e.g., PyTorch Geometric, DGL) (Dwivedi et al., 2023; Hu et al., 2020), adhering strictly to published protocols and hyperparameter tuning recommendations for a fair comparison.

C.3 TRAINING PROCEDURE

All models were trained following a rigorous, standardized training protocol to ensure fair and comparable evaluations across different methods and datasets:

- **Optimizer:** Adam with initial learning rates tuned in the range [0.001, 0.01]. The default best-performing value was typically 0.005 across datasets.
- **Weight Initialization:** Xavier initialization was uniformly applied to all models.
- **Epochs and Early Stopping:** Training was conducted for a maximum of 300 epochs, with early stopping activated based on validation performance to prevent overfitting (patience = 30 epochs).
- **Learning Rate Scheduler:** ReduceLROnPlateau scheduler was employed with a reduction factor of 0.5 and patience of 10 epochs.
- **Regularization:** Standard regularization techniques such as dropout (rates tuned from [0.1, 0.5]) and L2 weight decay (values tuned from $[10^{-4}, 10^{-3}]$) were employed across models.

For experiments involving our proposed SCA regularization, we trained each baseline model twice—once without SCA (standard baseline) and once with SCA integrated into the loss function. We tuned the regularization parameter λ from the range [0.01, 1.0], ultimately selecting $\lambda = 0.1$ as the optimal value balancing structural error uniformity and predictive performance.

Hyperparameter optimization was performed using grid search on validation sets, and the final reported results are averages over five independently repeated runs with different random seeds, ensuring the statistical robustness of our conclusions.

D FURTHER DISCUSSION

In this section, we provide a quantitative example to illustrate the limitations of existing GNN evaluation metrics, and we discuss how our proposed framework can be extended to capture spatial-temporal applications and other structural patterns.

D.1 QUANTITATIVE EXAMPLE (TRAFFIC MANAGEMENT)

Consider two GNN models, Model I and Model II, tasked with predicting traffic flow in a city, measured in vehicles per hour (vph).

Model I:

- Errors occur at k nodes, with a prediction error of 10 vph per node.

1026 • The error distribution is uniformly spread across the network.
 1027

1028 **Model II:**

1029
 1030 • Errors occur at k nodes, with a prediction error of 6 vph per node.
 1031 • The error distribution is spatially clustered at critical regions or intersections.
 1032

1033 While traditional metrics like Mean Squared Error (MSE) would favor Model II due to its lower
 1034 average error, our proposed Structural Cluster Statistic (SCS) metric, which quantifies the structural
 1035 clustering of errors, would flag Model II as performing worse due to the concentration of errors in
 1036 critical areas.

1037 **Practical Implication** Consider a critical intersection with a maximum capacity of 50 vph, fed by
 1038 two adjacent roads, A and B, each expected to contribute 20 vph:

1040 **Model I (uniform errors):**

1041
 1042 • Makes a large error (+10 vph) only on Road A, while accurately predicting traffic flow on
 1043 Road B.
 1044 • **Result:** The total flow remains 50 vph (i.e., $20 + 30 = 50$), avoiding congestion.
 1045

1046 **Model II (clustered errors):**

1047
 1048 • Makes smaller errors (+6 vph) simultaneously on both Roads A and B.
 1049 • **Result:** The total flow exceeds capacity (i.e., $26 + 26 = 52$ vph), causing congestion,
 1050 despite the smaller individual errors.
 1051

1052 This example illustrates how traditional metrics like MSE can favor models with lower average er-
 1053 rors while overlooking critical operational risks. In contrast, our structure-aware SCS metric reveals
 1054 the potential dangers of spatially clustered errors, offering a more nuanced evaluation.

1055 **D.2 FURTHER EXTENSION OF OUR FRAMEWORK**

1056 Our proposed evaluation framework, particularly the Spatial Cluster Statistic (SCS), is highly adapt-
 1057 able and can be extended to capture a wide range of spatial and structural error patterns beyond
 1058 basic spatial clustering. In this section, we discuss several potential extensions of our framework,
 1059 including how it can be adapted to detect errors related to spatial boundaries, directional biases, and
 1060 temporal dependencies.

1061 **Boundary Errors** In many spatial tasks, errors near the boundaries of the graph may have a sig-
 1062 nificantly different impact compared to errors in the interior. For example, in urban planning or envi-
 1063 ronmental monitoring, boundary regions—such as city borders or edges of monitored areas—might
 1064 have higher error tolerance or greater sensitivity. To address this, we can modify the weight assign-
 1065 ments in our framework to give higher importance to errors occurring at boundary nodes, ensuring
 1066 that our metric appropriately reflects the unique challenges of these critical areas.
 1067

1068 **Directional Biases** In certain applications, spatial directionality plays a key role in error distribu-
 1069 tion. For instance, in traffic flow predictions, errors may be more significant in certain directions
 1070 (e.g., towards city centers during rush hour) compared to others. Our framework can be extended by
 1071 assigning distinct weights based on the spatial direction of errors, allowing it to capture directional
 1072 biases in prediction errors. This adaptation is particularly useful in modeling scenarios where spatial
 1073 dependencies are not just local but also directional, such as weather patterns or traffic management.
 1074

1075 **Temporal Dependencies** Many real-world applications, such as traffic forecasting or environ-
 1076 mental monitoring, involve dynamic systems where prediction errors evolve over time. To adapt our
 1077 framework to such spatial-temporal settings, we can modify the weight assignment in Equation (3.1)
 1078 to incorporate temporal dependencies. This adaptation would account for both spatial and temporal
 1079

1080 proximity of errors, giving higher correlation weights to errors that occur closer in time. By incorporating
1081 temporal dependencies, our framework can capture how prediction errors evolve over time,
1082 providing more comprehensive evaluations in dynamic applications.

1083 For example, in traffic prediction, errors at a given intersection may not only depend on the spatial
1084 proximity to other intersections but also on how traffic conditions change over time. This temporal
1085 extension makes our metric applicable to a wider range of applications involving dynamic systems.
1086

1087 **Generalizing to Other Structural Error Patterns** Beyond spatial and temporal dependencies,
1088 our framework can be generalized to handle other structural error patterns by adjusting the weighting
1089 scheme. For instance, we can extend the metric to handle errors occurring along specific boundaries
1090 or errors that exhibit non-random patterns due to topological features of the graph, such as hub-
1091 based or scale-free structures. These extensions allow our framework to be applied in a wide range
1092 of contexts, including social networks, recommendation systems, and sensor networks, where the
1093 underlying graph structure significantly influences the error distribution.

1094 In summary, our framework is highly flexible and can be extended to capture a variety of error pat-
1095 terns, including boundary effects, directional biases, and temporal dependencies. These extensions
1096 enhance the applicability of our evaluation metric in more complex, real-world scenarios, providing
1097 richer insights into model performance.

1098

1099

1100

1101

1102

1103

1104

1105

1106

1107

1108

1109

1110

1111

1112

1113

1114

1115

1116

1117

1118

1119

1120

1121

1122

1123

1124

1125

1126

1127

1128

1129

1130

1131

1132

1133